

## CASE REPORT

Akihiro Hemmi · Akira Komiyama · Shinichi Ohno  
Yasuhisa Fujii · Ryohei Katoh · Akira Yokoyama  
Akira Kawaoi

## Poorly differentiated desmin-negative and vimentin-positive leiomyosarcoma of the stomach examined by the immunohistochemical and quick-freezing and deep-etching methods

Received: 28 May 1997 / Accepted: 15 September 1997

**Abstract** A poorly differentiated leiomyosarcoma of the stomach in a 41-year-old woman is reported. The diagnosis was confirmed by the diffuse immunohistochemical reaction to HHF35, and the presence of focal density and caveolas in some of the tumour cells by conventional electron microscopy. Immunohistochemically, most tumour cells had an undifferentiated nature, in which negative immunostaining for desmin, alpha-smooth muscle actin, and type IV collagen, and positive immunostaining for vimentin were observed. By the quick-freezing and deep-etching (QF-DE) method, these tumour cells revealed the loss of bundled actin and myosin filaments, which constitute desmin associated structures (focal densities and dense patchy areas). Their cytoplasm had many mitochondria and other cell organelles. The intermediate filaments (IFs), which were determined to be vimentin by immunohistochemistry, were observed in the inter-organellar spaces, and connected with these cell organelles. Actin filaments formed a meshwork structure and were distributed mainly in subplasmalemmal regions. Although a basal lamina was not detected by conventional electron microscopy, basal lamina-like structures, an association between the extracellular matrices and the cell membrane, were observed. Using the QF-DE method, three dimensional ultrastructural alterations of the cytoskeleton and extracellular matrix of the leiomyosarcoma were observed.

**Key words** Leiomyosarcoma · Stomach · Immunohistochemistry · Quick-freezing · Deep-etching

### Introduction

In pathological diagnosis ultrastructural investigation is often useful. There has been no report of human materials examined for pathological diagnosis with the quick-freezing and deep-etching (QF-DE) method an advanced morphological technique by which the three-dimensional ultrastructures can be observed at high resolution [3, 10, 16, 17, 25, 28].

We examined a poorly differentiated desmin-negative and vimentin-positive leiomyosarcoma of the stomach by the QF-DE method. A three-dimensional ultrastructural change in the tumour cells was reported with the immunohistochemical and conventional ultrastructural findings.

### Clinical history

A 41-year-old Japanese woman was admitted to Tokuji hospital with a complaint of general fatigue on 16 September 1995. The patient had noticed abdominal distension about 2 weeks before. A gastric tumour was suspected after gastric endoscopy and abdominal ultrasonography. For further examination of the gastric tumour, she was transferred to the second surgery department of Yamanashi Medical University Hospital. Physical examination revealed a smooth and removable tumour about 10 cm in diameter with a soft consistency on the left side of the abdomen. The CT scanner image revealed a huge abdominal tumour, 17×12×17 cm in size. As determined by gastric endoscopy, it was a submucosal tumour of her stomach, and a pathological diagnosis of spindle cell sarcoma was made on the gastric biopsy specimens. Laboratory studies disclosed no other abnormality. Total gastrectomy with pancreatosplenectomy and lymphonectomy was done on 6 November 1995. After the operation, additional chemotherapy was performed. The patient was discharged from the hospital on 20 December 1995. Her past and family histories were noncontributory.

### Materials and methods

A portion of the gastric tumour was used for conventional electron microscopy and the QF-DE method. For the light microscopic examination, the tumour tissue was fixed in 10% buffered formalin solution, processed according to standard methods, and embedded in paraffin.

A. Hemmi (✉) · A. Komiyama · R. Katoh  
A. Yokoyama · A. Kawaoi  
Second Department of Pathology, Yamanashi Medical University,  
1110 Shimokato, Tamaho-cho, Nakakoma-gun,  
Yamanashi 409-38, Japan  
Fax: (+81) 552-73-7108

S. Ohno · Y. Fujii  
Department of Anatomy, Yamanashi Medical University,  
Yamanashi, Japan

**Table 1** Primary antibodies used in this study (*MoAb* monoclonal antibody, *PoAb* polyclonal antibody, – negative reactivity, + mild, ++ intense)

Antibodies	Source	Clonality	Dilution	Reactivity
HHF35	DAKO Japan, Kyoto, Japan	MoAb	1:50	++
Desmin	DAKO Japan	PoAb	1:50	–
Myoglobin	DAKO Japan	PoAb	1:100	–
Myosin	Zymed Laboratories, South San Francisco, Calif.	PoAb	1:50	–
Vimentin	DAKO Japan	MoAb	1:50	++
S-100 protein	DAKO Japan	PoAb	1:50	–
HAM-56	DAKO Japan	MoAb	1:50	–
alpha-1-antitrypsin	DAKO Japan	PoAb	1:50	–
Type IV collagen	LSL, Tokyo, Japan	PoAb	1:1000	–
$\alpha$ -SMA	DAKO Japan	MoAb	1:40	–
CD34	Immunotech	MoAb	1:50	+

For the QF-DE method, small fragments of the tumour tissue were fixed with 2% paraformaldehyde in 0.1 M phosphate buffer (PB), pH 7.2. They were further cut into several pieces (5×3×2 mm in size) with sharp razor blades. To remove the soluble substances from the surface of the tissue, they were washed in PB for 30 min. They were postfixed with 0.25% glutaraldehyde in PB for 30 min and rinsed in 10% methanol to minimize ice crystal formation during the subsequent quick-freezing step. The tissue was placed on a copper metal holder with the cut tissue surface up and blotted with filter paper to remove excess fluid. The specimens were then quickly frozen by the metal contact method using a quick-freezing machine (JEOL JFD-RFA, Japan), in which the copper metal was cooled by liquid nitrogen (–196°C). They were freeze-fractured in the liquid nitrogen with a scalpel to expose the well-preserved tissue surface areas [25, 28] and transferred into an EIKO FD-3AS etching machine (Eiko Company, Ibaragi, Japan). They were deeply etched under vacuum conditions ( $1 \sim 4 \times 10^{-7}$  Torr) at –95°C for 10–20 min and rotary-shadowed with platinum at an angle of 30° and with carbon at an angle of 90°. One drop of 2% collodion in amyl acetate was placed onto the replicas as soon as the specimens were taken out from the machine, to prevent from the replicas breaking into pieces during the following digestion procedure. The replicas, coated with dried collodion, were floated on household bleach (Haitei, Kao, Japan) for 15–30 min to dissolve the tissue components. The replica membranes were washed in distilled water and cut into small pieces with a pair of scissors. They were mounted on Formvar-filmed copper grids and immersed in amyl acetate solution to dissolve the dried collodion. All the replicas were observed using an electron microscope (Hitachi H-600) and photographed at various magnifications.

For conventional electron microscopy, the tumour tissue was cut into small pieces and fixed in 2.5% glutaraldehyde in PB for 2 h at 4°C. They were postfixed in 1% osmium tetroxide in PB for 2 h at 4°C and embedded in Epon 812. Ultrathin sections were stained with uranyl acetate and lead citrate and examined in the same electron microscope.

For immunohistochemistry, the staining procedure employed was the streptavidin-biotin method using the LSAB kit (Dako Japan, Kyoto, Japan). Antibodies used in this study are listed in Table 1. The preparation for the type IV collagen was pretreated with 0.4% pepsin (Sigma, St. Louis, Mo.) in 0.01 N HCl for 120 min at room temperature before the addition of the primary antibodies. Normal mouse or rabbit serum was used for controls instead of the primary antibodies.

## Results

The resected tumour had a soft consistency, and its size was 24×20×18 cm. It was attached to the gastric wall and covered with gastric mucosa (Fig. 1a). There were two small ulcers at the centre of its mucosal surface. The tumour tissue contained scattered foci of necrosis and

haemorrhage, which continued to the muscle layer on the cut tissue surface (Fig. 1a). Histologically, the tumour consisted of spindle cells with moderately hyperchromatic, elongated, and blunt-edged nuclei, and small amounts of eosinophilic cytoplasm with unclear cell borders (Fig. 1b). The tumour cells were arranged in a fascicle or whorl pattern. Anisonucleosis and mitosis were prominent (Fig. 1c). At the periphery of the tumour infiltrating growth into the surrounding soft tissue was also detected.

The immunohistochemical results are summarized in Table 1. Most tumour cells had a positive immunoreaction to HHF35 and vimentin (Fig. 1d, e), and a weak immunoreaction to CD34 was observed focally. The monoclonal antibody for HHF35 has been previously characterized to recognize the  $\alpha$  and  $\gamma$  isotypes of actin, which are specific for muscle cells [31]. Immunoreactivity for desmin, myosin, and alpha smooth muscle actin ( $\alpha$ -SMA) was not seen in the tumour cells. The S-100 protein and HAM-56 and alpha-1-antitrypsin, which are hallmarks of neurogenic and fibrohistiogenic differentiation, respectively [2, 7, 12, 19, 22, 24], had negative immunoreactions. Type IV collagen and myoglobin also had a negative immunoreaction.

Electron microscopy showed that the tumour cells had a spindle configuration but their shape was extremely irregular compared with a normal smooth muscle cell. They had occasional cytoplasmic processes. The nuclei had infoldings of the nuclear membranes and increased chromatins distributed at the nuclear periphery (Fig. 2a). There were many mitochondria, various amounts of rough-surfaced endoplasmic reticulum (rER), polysomes and glycogen granules (Fig. 2b). In most of the tumour cells, as revealed on the replica membranes, their cytoplasm contained irregular networks of intermediate filaments (IF) that were 10 nm thick, but the bundled arrangement of thin (actin) and thick (myosin) filaments was not so conspicuous. Some IFs were connected with nuclei, mitochondria, and other cell organelles (Fig. 2c). Microfilaments were also observed, but they formed irregular meshwork structures, which consisted of thinner filaments 5 nm thick and located in the subplasmalemmal regions (Fig. 2d). A few well-differentiated tumour cells were seen in the conventional ultrathin sections (Fig. 2e) to have caveolas along the cell membrane and a focal density in their cytoplasm. Characteristic features,

**Fig. 1a-e** Gross and histological appearance of the tumour. **a** A submucosal tumour with haemorrhage and necrosis is covered with gastric mucosa. The tumour arises from the muscular layer, and a small central ulcer is seen at the mucosal surface. **b** Fascicular arrangement of the spindle tumour cells is seen. HE,  $\times 112$ . **c** The tumour cells have eosinophilic cytoplasm with indistinct cell borders, and hyperchromatic, elongated and blunt-edged nuclei. Anisonucleosis and mitosis are prominent. HE,  $\times 223$ . Immunohistochemical staining for **d** HHF35 and **e** vimentin. Streptavidin-biotin method,  $\times 112$ . The tumour cells show a positive immunoreaction to HHF35 and vimentin. Endothelial cells in the small vessels (**e**, upper side) also reveal positive immunoreaction for vimentin

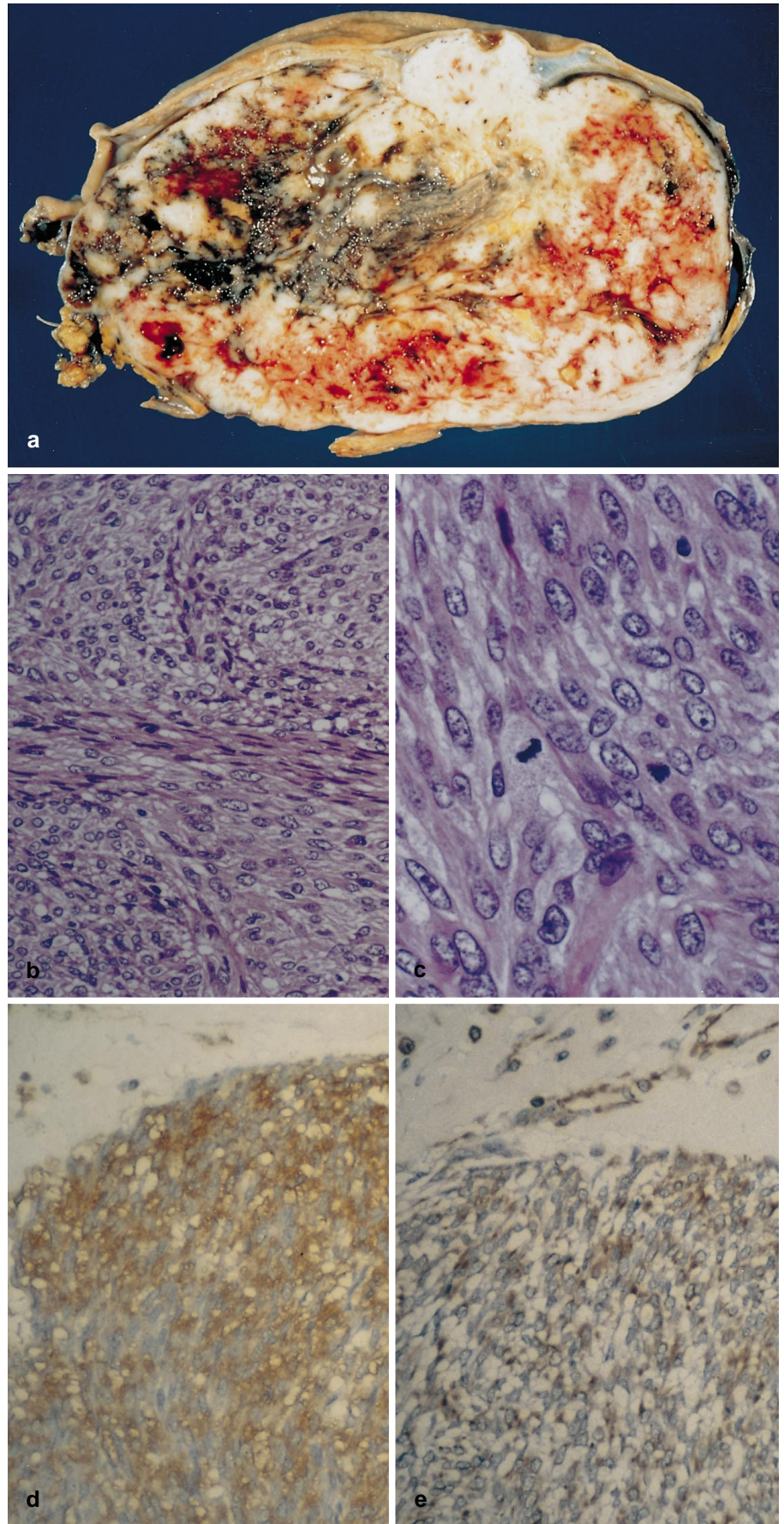




**Fig. 2a–f** Electron micrographs of the tumour cells, as revealed by the conventional electron microscopy and the QF-DE method. **a** Tumour cells show the spindle configuration, but their cytoplasm and nuclei are irregular (ultrathin section). **b** There are many mitochondria (*M*) in the cytoplasm. Note the network of intermediate filaments in the inter-organellar spaces in the *right micrograph* of the replica membrane. *Left micrograph*; corresponding area of ultrathin sections (*N*; nucleus). **c** Intermediate filaments are interconnected with mitochondria (*M*) and other cell organelles (replica membrane). **d** Irregular meshworks of microfilaments (*small arrows*) are located in the subplasmalemmal regions of the cytoplasm. Intermediate filaments (*large arrows*) are also observed. (replica membrane, *CS* cytoplasmic surface). **e** Caveolae (*arrowheads*) on the cell membrane and focal densities (*arrows*) in the cytoplasm (*right electron micrograph*) are noted in the well-differentiated tumour cell (*left electron micrograph*; ultrathin section). **f** A fine network in the extracellular matrix (*arrowheads*) is associated with the cell surface. In the region of the cytoplasmic processes (*arrow*) there is little association between the cell surface and the extracellular matrix (replica membrane). *Inset*; corresponding area of ultrathin sections

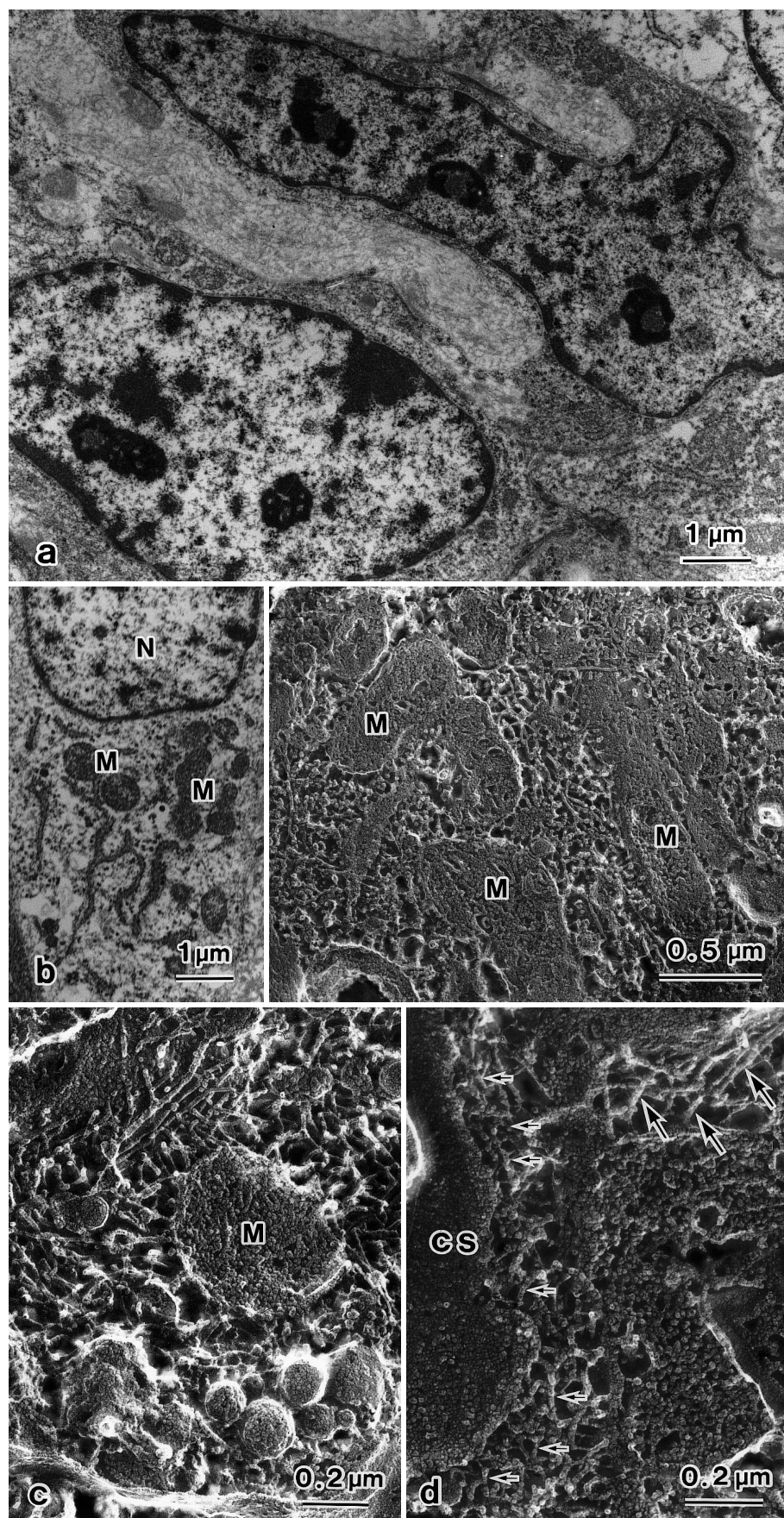
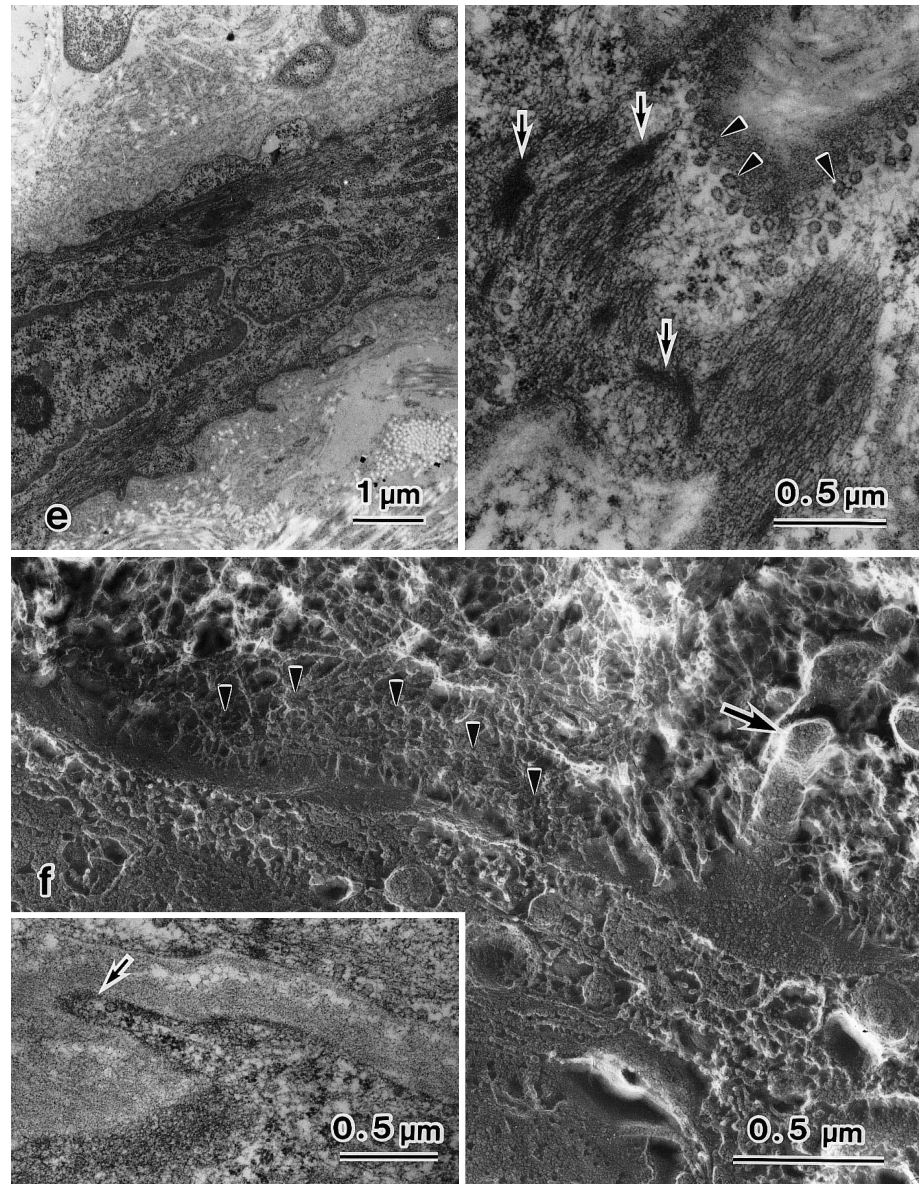


Fig. 2e-f



which suggested both myofibroblastic or fibrous histiocytoma cells (well-developed rER, many lysosomes, erythro- and/or haemosiderophagocytotic vacuoles, and pseudo- or filo-podia) [2, 11, 33, 36], and peripheral nerve stromal tumour cells (interdigitating long cytoplasmic processes joined by primitive cell junctions, scattered neurotubules, and neurosecretory dense-cored granules) [6, 14, 15], were not observed in the tumour.

A basal lamina around each tumour cell was not revealed by conventional electron microscopy, but networks of filaments in the extracellular matrices were associated with the focal areas of its cell membrane (Fig. 2f). The QF-DE method demonstrated that the basal lamina was a network of type IV collagen, laminin, and heparan sulfate proteoglycans [1], which was connected with the cell surface by the anchoring short filaments that traversed the lamina lucida [1]. In the present case, this basal lamina-like structure was observed on the replica membrane.

## Discussion

This is a case of a nonepithelial malignant neoplasm of the stomach. In addition to the atypical morphological features, the negative immunostaining for  $\alpha$ SMA, desmin, and type IV collagen and alternative positive immunostaining for vimentin suggested that most of the tumour cells were undifferentiated. However, focal densities and caveolae were recognized in a few tumour cells, which did not have a well-developed rER. These electron microscopic findings, and the positive immunoreaction to HHF35, demonstrated that the tumour had smooth muscle, but not myofibroblast, differentiation. No immunoreaction to S-100 protein, HAM-56 or alpha-1-antitrypsin, and no electron microscopical features indicating fibrohistiocytic or peripheral nerve differentiation were seen. We therefore did not diagnose the lesion as a malignant fibrous histiocytoma or malignant peripheral

nerve stromal tumour, but rather as a poorly differentiated leiomyosarcoma.

For many years, spindle and/or epithelioid stromal tumours of the gastrointestinal tract were regarded as being basically of a smooth muscle nature. Many immunohistochemical and ultrastructural studies in recent years have shown a more complex histogenesis, and they are now referred to as gastrointestinal stromal tumours (GISTs) [6, 9, 18, 29, 30, 34]. GISTs are thought to comprise a heterogeneous group of nonepithelial tumours with different cell origins and various degrees of differentiation. In Ackerman's surgical pathology textbook [29] and other reports [4, 18, 26, 34], GISTs are divided into four major categories on the basis of their phenotypical features: tumours with smooth muscle differentiation (smooth muscle type), tumours with neural differentiation (neural type), tumours with bi-directional muscular/neural differentiation (smooth muscle-neural type), and tumours without differentiation (uncommitted type), a high percentage of which show an immunoreactivity to CD34, a myeloid progenitor cell antigen [23, 35]. We decided that the present tumour is a malignant GIST, a smooth muscle type. The undifferentiated nature of most tumour cells reflects CD34 immunoreactivity.

The three-dimensional ultrastructural features were examined by the QF-DE method. Typical well-organized filaments with bundle formation, as seen in a normal smooth muscle cell [27], were not observed in the cytoplasm of most of the tumour cells. Instead, there was a marked increase of mitochondria and other cell organelles. Actin filaments were distributed in the subplasmalemmal regions of the cytoplasm, and they formed an irregular meshwork structure without definite myosin filaments (15 nm in diameter). These results indicated that the actin filaments in the tumour cells play a part in the support provided by the cell membrane, but not in muscle contraction. The focal densities and dense patches are special regions, in which the actin filaments are interconnected with the desmin IFs in the bundles, and are attached to the cell membrane, respectively [32]. The caveolae have a role in the absorption of calcium ions, which is necessary for muscle contraction [5]. Unlike desmin IF, which mainly support the contraction proteins, vimentin IF has been reported to support cell organelles and nuclei [20, 21]. The disappearance of the bundled arrangement of the cytoskeleton, which is a differentiated structure used for the contraction of smooth muscle cells, is thought to be an essential change in neoplastic transformation. These changes of the cytoskeleton and cell organelles might be related to the disappearance of the focal densities, dense patches, and caveolae, and also to the altered expression of desmin or vimentin in the tumour cells. The basal lamina is one of the ultrastructural findings that characterizes a smooth muscle cell origin [8, 13], but in the present case basal lamina was not detected along the cell membrane of most of the tumour cells by conventional electron microscopy. The networks of basal lamina-like structures in the extracellular matrices were easily observed on the replica membranes.

There are reports regarding the immunohistochemical changes of the cytoskeleton and extracellular matrix of the leiomyosarcoma [9, 30], but the ultrastructural features corresponding to the immunohistochemical changes remain obscure. Using the QF-DE method, the alterations of the cytoskeleton and extracellular matrix, which were not easily observed by conventional electron microscopy, could be clearly observed. We conclude that this method is useful for the pathological examination for surgical materials and also for experimental research. Further investigation of surgical materials using the QF-DE method is needed.

## References

- Adachi E Hayashi T (1994) Anchoring of epithelia to underlying connective tissue: evidence of frayed ends of collagen fibrils directly merging with meshwork of lamina densa. *J Electron Microsc* 43:264–271
- Adams CW, Poston RN (1990) Macrophage histology in paraffin-embedded multiple sclerosis plaques is demonstrated by the monoclonal pan-macrophage marker HAM-56: correlation with chronicity of the lesion. *Acta Neuropathol* 80:208–211
- Baba T, Shiozawa N, Hotchi M, Ohno S (1991) Three-dimensional study of the cytoskeleton in macrophages and multinucleate giant cells by quick-freezing and deep-etching method. *Virchows Arch [B]* 61:39–47
- Brainard JA, Goldblum JR (1997) Stromal tumours of the jejunum and ileum: a clinicopathologic study of 39 cases. *Am J Surg Pathol* 21:407–416
- Devine CE, Somlyo AV, Somlyo AP (1972) Sarcoplasmic reticulum and excitation-contraction coupling in mammalian smooth muscles. *J Cell Biol* 52:690–718
- Dhimes P, López-Carreira M, Ortega-Serrano MP, García-Muñoz H, Martínez-González MA, Ballestín C (1995) Gastrointestinal autonomic nerve tumours and their separation from other gastrointestinal stromal tumours: an ultrastructural and immunohistochemical study of seven cases. *Virchows Arch* 426:27–35
- duBoulay G (1982) Demonstration of alpha-1-antitrypsin and alpha-1-antichymotrypsin in fibrous histiocytomas using the immunoperoxidase technique. *Am J Surg Pathol* 6:559–564
- Enzinger FM, Weiss SW (1988) *Soft tissue tumours*, 2nd edn. Mosby, St. Louis Washington DC Toronto, pp 402–421
- Franquemont DW, Frierson Jr HF (1992) Muscle differentiation and clinicopathologic features of gastrointestinal stromal tumours. *Am J Surg Pathol* 16:947–954
- Furuta K, Ohno S, Gibo Y, Kiyosawa K, Furuta S (1992) Three-dimensional ultrastructure of normal rat hepatocytes by quick-freezing and deep-etching method. *J Gastroenterol Hepatol* 7:486–490
- Gabbiani G, Majno G (1972) Dupuytren's contracture: fibroblastic contraction? An ultrastructural study. *Am J Pathol* 66:131–146
- Gown AU, Tsukada T, Ross R (1986) Human atherosclerosis II. Immunocytochemical analysis of the cellular composition of human atherosclerotic lesions. *Am J Pathol* 125:191–207
- Hashimoto H, Daimaru Y, Tsuneyoshi M, Enjoji M (1986) Leiomyosarcoma of the external soft tissues. A clinicopathologic, immunohistochemical, and electron microscopic study. *Cancer* 57:2077–2088
- Herrera GA, Pinto de Moraes H, Grizzle WE, Han SG (1984) Malignant small bowel neoplasm of enteric plexus derivation (plexosarcoma): light and electron microscopic study confirming the origin of the neoplasm. *Dig Dis Sci* 29:275–284
- Herrera GA, Cerezo L, Jones JE, Sack J, Grizzle WE, Pollack WJ, Lott RL (1989) Gastrointestinal autonomic nerve tumours. *Arch Pathol Lab Med* 113:846–853

16. Heuser JE, Kirschner MW (1980) Filament organization resolved in platinum replicas of freeze-dried cytoskeleton. *J Cell Biol* 86:212–234
17. Hirokawa N, Heuser JE (1981) Quick-freeze, deep-etch visualization of the cytoskeleton beneath surface differentiations of intestinal epithelial cells. *J Cell Biol* 91:399–409
18. Hurlimann J, Gardiol D (1991) Gastrointestinal stromal tumours: an immunohistochemical study of 165 cases. *Histopathology* 19:311–320
19. Kindbloom L, Jacobsen G, Jacobsen M (1982) Immunohistochemical investigation of tumours of supposed fibroblastic-histiocytic origin. *Hum Pathol* 13:834–840
20. Lehto VP, Virtanen I, Kurki P (1978) Intermediate filaments anchor the nuclei in nuclear monolayers of cultured human fibroblasts. *Nature* 272:175–177
21. Lin A, Krockmalnic G, Penman S (1990) Imaging cytoskeleton-mitochondrial membrane attachments by embedment-free electron microscopy of saponin-extracted cells. *Proc Natl Acad Sci USA* 87:8565–8569
22. Meister P, Methras W (1980) Immunohistochemical markers of histiocytic tumours. *Hum Pathol* 11:300–301
23. Miettinen M, Virolainen M, Maarit-Sarlomo-Rikala (1995) Gastrointestinal stromal tumours – Value of CD 34 antigen in their identification and separation from true leiomyomas and schwannomas. *Am J Surg Pathol* 19:207–216
24. Nakajima T, Watanabe S, Sato Y, Kameya T, Hirota T, Shimamoto Y (1982) An immunoperoxidase study of S-100 protein distribution in normal and neoplastic tissues. *Am J Surg Pathol* 6:715–727
25. Naramoto A, Ohno S, Furuta K, Itoh N, Nakazawa K, Nakano M, Shigematsu H (1991) Ultrastructural studies of hepatocyte cytoskeletons of phalloidin-treated rats by quick-freezing and deep-etching method. *Hepatology* 13:222–229
26. Newman PL, Wadden C, Fletcher CDM (1991) Gastrointestinal stromal tumours: Correlation of immunophenotype with clinicopathological features. *J Pathol (Lond)* 164:107–117
27. Ogawa K, Mizoguchi F (1993) *Histology* (in Japanese), 2nd edn. Bunkodo, Tokyo, pp 194–200
28. Ohno S, Fujii Y (1991) Three-dimensional studies of the cytoskeleton of cultured hepatocytes: a quick-freezing and deep-etching study. *Virchows Arch [A]* 418:61–70
29. Rosai J (1996) Gastrointestinal tract. In: Ackerman's surgical pathology, 8th edn, vol. 1. Mosby, St. Louis, pp 645–647
30. Tirabosco R, Cavazzana AO, Santeusanio G, Spagnoli LG (1995) Gastrointestinal stromal tumour: evidence for a smooth-muscle origin. *Mod Pathol* 8:193–196
31. Tsukada T, McNutt MA, Ross R, Gown AM (1987) HHF35, a muscle actin-specific monoclonal antibody II. Reactivity in normal, reactive, and neoplastic human tissues. *Am J Pathol* 127:389–402
32. Tsukita S, Tsukita S, Ishikawa H (1983) Association of actin and 10-nm filaments with the dense body in smooth muscle cells of the chicken gizzard. *Cell Tissue Res* 229:233–242
33. Tsuneyoshi M, Enjoji M, Shinohara N (1981) Malignant fibrous histiocytoma: an electron microscopic study of 17 cases. *Virchows Arch [A]* 392:135–145
34. Tworek JA, Appelman HD, Singleton TP, Greenson JK (1997) Stromal tumours of the jejunum and ileum. *Mod Pathol* 10:200–209
35. Van De Rijn M, Hendrickson MR, Rouse RV (1994) CD34 expression by gastrointestinal tract stromal tumours. *Hum Pathol* 25:766–771
36. Yang P, Hirose T, Seki K, Hasegawa T, Hizawa K, Sano T (1996) Myofibroblastic tumour of soft tissue displaying desmin-positive and actin-negative immunophenotypes. *Pathol Int* 46:696–703